Chinese Chemical Letters 36 (2025) 110078

Contents lists available at ScienceDirect

Chinese Chemical Letters

journal homepage: www.elsevier.com/locate/cclet

A novel photocatalytic mechanism of volatile organic compounds degradation on $BaTiO_3$ under visible light: Photo-electrons transfer from photocatalyst to pollutant

Teng Wang[a,1], Jiachun Cao[a,b,1], Juan Li[b], Didi Li[a], Zhimin Ao[b,*]

[a] Guangdong-Hong Kong-Macao Joint Laboratory for Contaminants Exposure and Health, Guangdong Key Laboratory of Environmental Catalysis and Health Risk Control, Key Laboratory for City Cluster Environmental Safety and Green Development of the Ministry of Education, Institute of Environmental Health and Pollution Control, School of Environmental Science and Engineering, Guangdong University of Technology, Guangzhou 510006, China
[b] Advanced Interdisciplinary Institute of Environment and Ecology, Guangdong Provincial Key Laboratory of Wastewater Information Analysis and Early Warning, Beijing Normal University, Zhuhai 519087, China

ARTICLE INFO

Article history:
Received 5 January 2024
Revised 17 April 2024
Accepted 31 May 2024
Available online 1 June 2024

Keywords:
Volatile organic compounds
Photocatalytic Degradation
Wide-bandgap semiconductors
Density functional theory
Degradation mechanism

ABSTRACT

Wide bandgap semiconductors are typically activated under ultraviolet (UV) light irradiation for volatile organic compounds (VOCs) degradation. However, our previous study discovered that certain VOCs can interact with some wide bandgap semiconductors, formatting an intermediate bandgap between the VOCs and the conduction band of wide bandgap semiconductor, thus inducing visible light activation of the system, and photo-generated electrons are excited by visible light and transferred from the VOCs to the conduction band of semiconductor. In this work, $BaTiO_3$, traditionally is not active under visible light irradiation, however showed degradation rates of 100% and 20% for styrene and toluene under visible light, respectively. Density functional theory (DFT) calculations indicate that the adsorption of styrene or toluene on the $BaTiO_3$ surface reduces its bandgap from 2.93 eV to 1.36 eV and 2.26 eV, respectively. The intermediate bandgap in this system is primarily formed by the valence band of $BaTiO_3$ and the VOCs, and indicating that photo-generated electrons directly transfer from $BaTiO_3$ to the VOCs under visible light, inducing degradation reactions of VOCs, *i.e.*, this work discovered a new transfer pathway of photo-electrons direct from the valence band of $BaTiO_3$ to VOCs, while photo-electrons are from VOCs to the conductive band of wide-bandgap semiconductors in our previous work.

Volatile organic compounds (VOCs) are a major source of air pollution, profoundly impacting both ecological environments and human health [1-3]. Consequently, developing efficient and practical technologies to eliminate VOCs is of critical importance. In recent years, based on the traditional gas-solid phase photocatalytic mechanism [4], the photocatalytic degradation of VOCs has become a focal point in both research and application. The research focuses primarily on the development of high-performance catalysts [5-7], catalytic reactors [8-10], and integration with other technologies. Wide bandgap semiconductors are one type of most common photocatalysts, such as TiO_2, which require ultraviolet (UV) light to excite electrons in the valance band of the photocatalyst to the conduction band [11]. The development of high-performance catalysts mainly concentrates on modifying traditional wide bandgap semiconductors, such as through doping [12,13], constructing heterojunctions [14,15], and developing novel photocatalysts [11,16,17] in order to utilize the visible light.

Recently, our previous work reported an untraditional phenomenon that some unmodified wide bandgap semiconductors, such TiO_2, ZnO, and Ta_2O_5, can photodegrade VOCs under visible light irradiation, and a new photocatalytic mechanism of VOCs participating in the photo-generated electron process has been reported [18]. This unconventional photocatalytic mechanism suggests that the efficiency of light energy utilization in photocatalysts is not only related to the bandgap of the catalyst but also the VOCs being degraded. Specifically, an intermediate bandgap capable of utilizing visible light forms between VOCs and the conduction band of wide-bandgap semiconductor catalysts. Electrons transfer from the VOCs to the conduction band of the catalyst, further generating free radicals that attack pollutants. Consequently, there might exist an intermediate bandgap between the valence band of the wide-bandgap semiconductor and the VOCs, which can

* Corresponding author.
E-mail address: zhimin.ao@bnu.edu.cn (Z. Ao).
[1] These authors contributed equally to this work.

https://doi.org/10.1016/j.cclet.2024.110078
1001-8417/

utilize visible light, allowing photo-generated electrons to directly transfer from the valence band of the catalyst to the VOCs.

Traditionally, due to wide bandgap (3.2 eV) of $BaTiO_3$ and limited narrow light response confined to the UV light [19], its photocatalytic degradation efficiency was limited [20]. However, our research observed significant degradation of styrene and toluene under visible light, suggesting a potential new mechanism for the photocatalytic degradation of VOCs. Further studies revealed that, unlike previously reported catalysts forming narrower bandgaps at the position of the conduction band of catalyst with VOCs [18], a narrower bandgap formed at the valence band position with VOCs when styrene or toluene adsorbed on the $BaTiO_3$ surface. This intermediate bandgap resulted in the direct transfer of photogenerated electrons from $BaTiO_3$ to the VOCs in the visible light photocatalytic reaction process, which can be confirmed by both experiment and density functional theory (DFT) calculations evidences. This discovery not only deepens our understanding of this novel photocatalytic mechanism but also lays a solid foundation for future research based on this mechanism.

Barium titanate ($BaTiO_3$) (purity of 99.9% with the size of 100 nm) was purchased from Shanghai Macklin Biochemical Co., Ltd (China), and used without any purification.

X-ray diffraction (XRD; Germany) analysis was performed with a Bruker D8 ADVANCE diffractometer, using Cu Kα radiation (wavelength: 1.5406 Å). To determine the valence band positions of the catalysts, an X-ray photoelectron spectroscope (XPS, Shimadzu ESCA 3200, Japan) was used by Mg Kα radiation. The binding energies of elements were referenced to the C 1s peak at 284.6 eV. In order to obtain the UV–vis diffuse reflectance spectra, Shimadzu UV-3600 Plus spectrophotometer (Japan) was used, referencing against $BaSO_4$. Identification of the functional groups of samples was achieved through Fourier transform infrared spectroscopy (FT-IR) using a Nicolet iS10 instrument (America).

The photocatalytic performance of the samples was evaluated by monitoring the degradation of VOCs in a specially designed flat quartz glass reactor. Illumination was provided by a 300 W Xenon lamp, positioned 10 cm from the reactor. Depending on the experiment, a wavelength cut filter at 420 nm and bandpass filters at various wavelengths (DT 450, 475, 500, 520, 550, 600, and 650 nm) were employed. Typically, a predefined quantity of catalyst was placed in the reactor, followed by the infusion of VOCs at a constant initial concentration of 20 ± 1 ppmv, diluted with air, and introduced at a rate of 20 mL/min. Prior to light exposure, samples were kept in the dark to achieve gas-solid adsorption-desorption equilibrium. The residual concentrations of VOCs and CO_2 produced in exhaust gases were quantified using an online gas chromatograph (GC) equipped with a dual flame ionization detector (FID).

The conversion efficiency (η_1) and mineralization rate (η_2) of VOCs were calculated using the following equations:

$$\eta_1 = \frac{c_0 - c}{c_0} \times 100\,\% \tag{1}$$

$$\eta_2 = \frac{Q_1}{M \times Q_0} \times 100\,\% \tag{2}$$

where, c_0 and c are the concentration of VOCs in the inlet and outlet gas, respectively; Q_0 is the amounts of VOCs degraded, Q_1 is the amounts of CO_2 in the outlet gas, and M is the number of carbon atoms in a specific VOC molecule.

The absorption spectrum of the catalyst in the process of VOCs adsorption was collected by UV–Vis-NIR spectrophotometer with integrating sphere (Shimadzu, UV-3600 PLUS). Each experiment commenced with placing the catalyst in a specially designed gas-solid phase *in situ* reaction cell, which was then sealed. The catalyst was initially purged with nitrogen (N_2) at a flow rate of 20 mL/min for 20 min. Spectra were collected continuously until a stable curve was obtained. Subsequently, the gas input was switched to VOCs at the same flow rate for *in situ* absorption spectra gathering. The data acquisition occurred at a rate of 1 nm/s, covering the wavelength range of 200 to 800 nm.

The adsorption spectra of VOCs on synthetic adsorbents were obtained by *in situ* diffuse reflectance infrared Fourier transform spectroscopy (DRIFTS, Thermo Science Nicolet IS 10) and mercuric cadmium telluride (MCT) detector. Prior to each measurement, the sorbent was positioned in a porous grid at the base of a reflector cell with dual ZnSe windows, which was then sealed with a dome. The sorbent underwent a purging process at 150 °C for one hour under a nitrogen (N_2) flow of 20 mL/min. After cooling to 30 °C, the baseline spectrum of the adsorbent was recorded under N_2 flow, and then switched to VOCs at a flow rate of 30 mL/min for adsorption analysis. All FT-IR spectra are collected in the range of 4000–400 cm^{-1}, with a resolution of 4 cm^{-1}. Additionally, pyridine infrared (Py-IR) analysis was carried out using a Thermo Nicolet 380 FT-IR instrument. The samples underwent dehydration at 400 °C for two hours before being exposed to pyridine vapor at 40 °C.

All DFT calculations in this work were performed using VASP software [21] and Perdew-Burke-Ernzerhof (PBE) exchange correlation functional correction [22]. An energy cutoff of 400 eV was used for plane-wave basis expansion. For the structural relaxations, the convergence criteria of atomic forces and total energy were set as 0.03 eV/Å and 1×10^{-6} eV, respectively. The DFT-D3 method was applied to consider the van der Waals interactions for correcting the Kohn-Sham energies [23].

The adsorption energy E_{ads} of the VOC molecule on the surface of $BaTiO_3$ (001) was calculated by

$$E_{ads} = E_{VOCs+slab} - E_{slab} - E_{VOCs} \tag{3}$$

where $E_{VOCs+slab}$, E_{slad}, and E_{VOCs} are the total energy of the simulated slab with VOC adsorbed, the clean slab, and the isolated VOC molecule, respectively.

Results and discussion section: $BaTiO_3$ is employed for the photocatalytic degradation of styrene, toluene, benzene, and ethyl acetate under visible light (wavelengths exceeding 420 nm). Interestingly, the degradation efficiency of styrene reached 100% in 220 min by $BaTiO_3$ in visible light, which then decreased to 80% over the following 400 min, concurrently generating approximately 17 ppmv of CO_2 (Figs. 1a and b). In comparison, the degradation of toluene was around 40% in the initial 100 min, and reduced to about 10% in the subsequent 400 min, producing only trace amounts of CO_2. However, no significant photocatalytic degradation and CO_2 formation were observed for benzene and ethyl acetate. This observation is contrary to the traditional photocatalytic mechanisms [24], where $BaTiO_3$ is deemed ineffective in utilizing visible light [20].

To further interpret this phenomenon, XRD was conducted to explore the crystal structure of this industrial-grade $BaTiO_3$ (see Fig. 1c). No significant structural differences were found compared to the standard PDF card (hexagonal crystal structure, JCPDS 79–2263) [25] implying that this commercial-grade $BaTiO_3$ contains no notable impurities or crystal alterations.

Additionally, UV–vis diffuse reflectance testing was performed, identifying an absorption band edge at 394.7 nm (Fig. 1d). Through conversion, the bandgap was determined to be 3.14 eV, consistent with literature descriptions [26]. This further confirms that $BaTiO_3$ does not significantly absorb light with wavelengths more than 420 nm. The selective degradation of styrene and toluene under visible light photocatalysis of $BaTiO_3$ suggests a new mechanism for the photocatalysis of $BaTiO_3$. Our recent study showed that VOCs can affect the absorption of visible light by semiconductor catalyst, so that VOCs can be degraded by wide-gap semiconductor

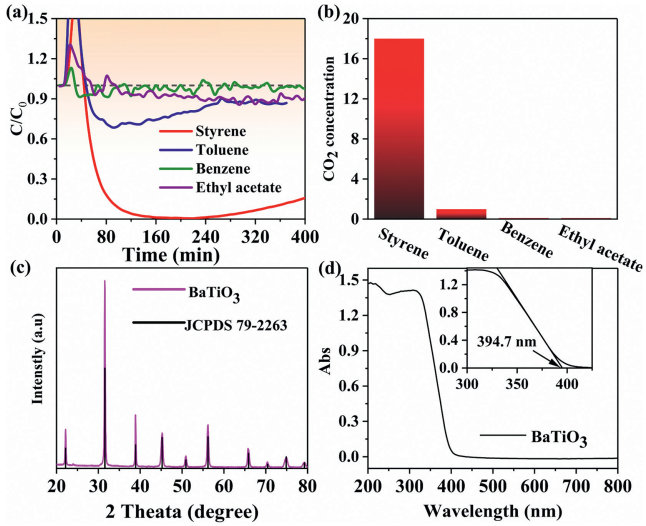

Fig. 1. (a) Degradation curves and (b) mineralization rate of $BaTiO_3$ for styrene, toluene, benzene and ethyl acetate under visible light. (c) XRD spectra of $BaTiO_3$ obtained in this work and from the PDF cards. (d) UV–vis diffuse reflection absorption pattern and absorption band edge of $BaTiO_3$.

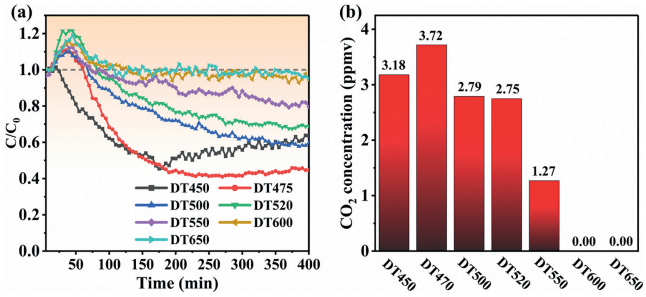

Fig. 2. (a) Photocatalytic degradation of styrene and (b) the amount of CO_2 produced by $BaTiO_3$ under different wavelengths of visible light.

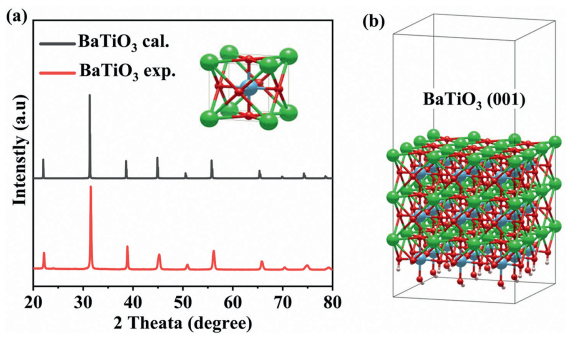

Fig. 3. (a) Comparison of the experimental and calculated powder diffraction pattern for investigated $BaTiO_3$ crystal. (b) The optimized structures of $BaTiO_3$ (001) surfaces.

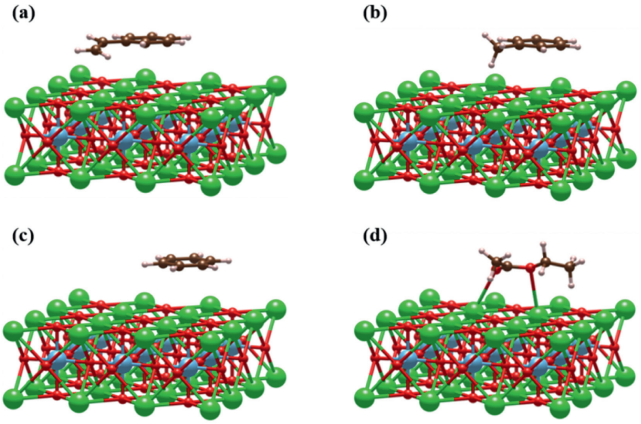

Fig. 4. The most stable structures of (a) styrene, (b) toluene, (c) benzene and (d) ethyl acetate adsorbing on the $BaTiO_3$ (001) surface, respectively.

Table 1
The adsorption energy (E_{ads}, eV) of VOCs molecules on $BaTiO_3$ (001) surface.

	Styrene	Toluene	Benzene	Ethyl-acetate
$BaTiO_3$ (001)	−0.732	−0.701	−0.602	−0.751

under visible light [18]. Hence, it is hypothesized that VOCs was involved in the $BaTiO_3$ photocatalytic oxidation of styrene.

To further validate our hypothesis, the photocatalytic degradation efficiency of $BaTiO_3$ on styrene across a range of visible light wavelengths (450, 470, 500, 520, 550, 600, and 650 nm) was investigated. As delineated in Fig. 2a, the photocatalytic degradation efficiency of $BaTiO_3$ for styrene remained relatively stable, with degradation rates oscillating between approximately 40%-50% under visible light wavelengths of 450 nm and 475 nm. Notably, the levels of CO_2 generated through the mineralization process were 3.18 ppmv and 3.72 ppmv under visible light wavelengths of 450 nm and 475 nm, respectively (Fig. 2b).

As the wavelength of the visible light increased, the degradation rate of styrene and the amount of CO_2 produced gradually decreased. Particularly, there was almost no discernible change in the concentration of styrene and CO_2 when the wavelength extended to 600 nm and 650 nm (Figs. 2a and b). These findings confirm that $BaTiO_3$ is indeed capable of effectively photocatalyzing the degradation of styrene under visible light. This provides a robust basis for further exploration into the underlying mechanisms at play.

DFT calculations have been employed to build the model of $BaTiO_3$ and investigate the coupling relationship between VOCs and $BaTiO_3$ in the photocatalytic degradation process. The initial phase and surface structures of $BaTiO_3$ are depicted in Fig. 3a. The calculated powder diffraction peaks exhibit favorable agreement with experimental data, suggesting that the crystal structure of these candidate materials well matches with that used in our experimental samples.

Subsequently, a (001) preferred slab was constructed based on the reshaped bulk structure, as previously confirmed. The periodic slab images are separated by a vacuum layer of at least 15 Å. The $2 \times 3 \times 1$ Monkhorst-Pack k-point mesh was employed to approximate sampling of the Brillouin zone. The Hubbard U parameter of 10.5 eV was used to consider the localized 3d electrons in Ti to better describe the band gap of $BaTiO_3$ crystal (Fig. 3b).

Furthermore, the adsorption behavior of VOCs on the $BaTiO_3$ (001) surface was thoroughly investigated. As depicted in Fig. 4, all VOCs molecules exhibit a stable adsorption on the metal sites of the surface, with adsorption energies ranging from −0.602 eV to −0.751 eV (Table 1). This favorable adsorption promotes the formation of interaction structures between VOCs molecule and the $BaTiO_3$ sample. Furthermore, the differential charge density reveals an accumulation of charge between the molecules and the adsorbed metal sites, facilitating the transfer of photo-generated electrons between the VOCs molecule and the $BaTiO_3$ (001) surface.

To ensure the consistency between the adsorption model constructed *via* DFT and the experimental data, an in-depth study using *in situ* DRIFTS and Py-IR for the adsorption of ethyl acetate on the surface of $BaTiO_3$ was conducted. Notably, DFT calculations indicated that only ethyl acetate forms significant chemical bonds

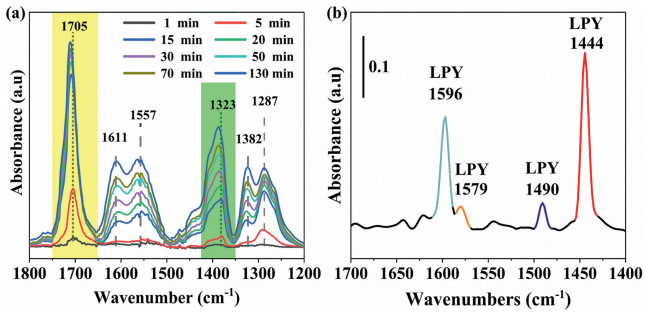

Fig. 5. (a) *in situ* DRIFTS spectra of ethyl acetate adsorbed onto $BaTiO_3$. (b) Py-IR spectra of $BaTiO_3$ at 30 °C.

with $BaTiO_3$, while other VOCs are chemically adsorbed on the $BaTiO_3$ surface (Fig. 4). Therefore, ethyl acetate was chosen as the object of the study. The *in situ* DRIFTS spectrum, presented in Fig. 5a, revealed prominent peaks at 1287 cm^{-1} and 1382 cm^{-1}, which are probably associated with the out-of-plane rocking and twisting vibrations of the -CH_2 group. Moreover, two pronounced bands were noted at 1557 cm^{-1} and 1611 cm^{-1}, indicating the asymmetric angular vibrations of the -CH_3 group. Notably, the intensification of these spectral peaks during the reaction implies an increasing presence of ethyl acetate on the $BaTiO_3$ surface. Bands at 1711–1705 cm^{-1} and 1387–1323 cm^{-1} corresponded to the stretching vibrations of aliphatic carbonyl (C=O) and ether linkage (C-O), respectively. The intensities of these absorption bands significantly increased over time, implying the possible formation of new chemical bonds at the C=O and C-O positions [27].

Additionally, the surface basicity of $BaTiO_3$ was determined using Py-IR analysis. Fig. 5b displays four distinct bands at 1444, 1490, 1579, and 1596 cm^{-1}, suggesting the chemisorption of pyridine on the Lewis acidic sites of the material [28,29]. This result unambiguously confirmed that pure $BaTiO_3$ possesses only Lewis acidic properties, substantiating that the metal Ba on the surface of $BaTiO_3$ serves as the primary adsorption site for VOCs (with no exposed Ti on the surface).

Therefore, the collective findings from *in situ* DRIFTS and Py-IR analyses corroborate that ethyl acetate adsorbs onto the Ba sites of $BaTiO_3$ *via* the two oxygen atoms of its aliphatic carbonyl group. This observation aligns closely with the adsorption model predicted by density functional theory (DFT) calculations. These findings robustly validate that the adsorption model constructed *via* DFT is consistent with experimental results, thereby lending credibility to conclusions drawn from this model.

To further elucidate the electronic transmission mechanism, the electronic structures of the adsorption system were calculated (Figs. 6 and 7). As shown in Fig. 7a, the result of the density of states (DOS) reveals that the adsorption of VOCs molecules induces additional unoccupied orbitals within the surface band gap. These unoccupied midgap states are the lowest unoccupied molecular orbital (LOMO) of the adsorbed molecules (Fig. 6). This could induce an electron transfer pathway from the $BaTiO_3$ (001) surface to VOCs molecules, consequently reducing the band gap of the semiconductor surface. The calculated absorption spectra of the $BaTiO_3$ (001) surface at ~400 nm are significantly enhanced after VOCs adsorption (Fig. S1 in Supporting information), confirming the decrease of surface band gap. Notably, this phenomenon is particularly pronounced in the case of styrene adsorption, which aligns with the experimental observation of enhanced visible light effects. Fig. 7b illustrates the electron transfer channels and their exciting energy. It demonstrates that the gap values from valence band maximum (VBM) of $BaTiO_3$ (001) to these unoccupied midgap states are located in the visible-light window (from 1.36 eV to

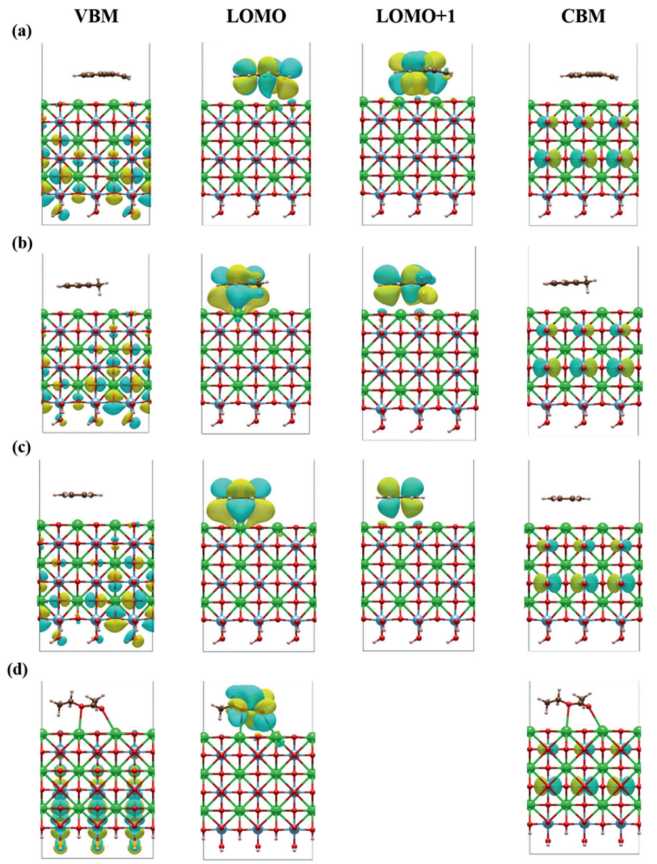

Fig. 6. The orbitals of $BaTiO_3$ (001) adsorption systems with adsorbing (a) styrene, (b) toluene, (c) benzene and (d) ethyl acetate, respectively.

2.91 eV), which is in agreement with the visible light response phenomenon observed in our experiments. As a result, the degradation of VOCs by $BaTiO_3$ under visible light, as studied, is anticipated to align with the charge transfer mechanism involving the midgap state and the frontier orbital on the semiconductor surface.

The photocatalytic efficiency of semiconductor surfaces adsorbed with VOCs can be assessed through energy level diagrams of key orbitals, as depicted in Fig. 7b. The result of band edges displays that there are midgap orbital closer proximity to the potential energy level generated by superoxide radical ($O_2^{\bullet-}$, −0.16 eV). This means that the photogenerated electrons activated from VBM to these midgap orbitals can react with O_2 to produce $O_2^{\bullet-}$. In particular, the lower than −0.16 eV LOMO orbital of styrene can be used as a transit station for photogenerated electrons, so that they can be activated to higher intermediate energy levels with lower energy (1.36 eV). Furthermore, the structures of VOC molecules alter negligibly after getting an electron (Table S1 in Supporting information), indicating that ingesting photoelectrons cannot directly lead to molecule photolysis. Fig. S1 illustrates that the midgap states formed post-adsorption of molecules on the $BaTiO_3$ (001) surface were localized on the adsorbed molecules. Simultaneously, the VBM of the semiconductor material was predominantly distributed within the material itself. This suggests that the electrons and holes produced by irritation are separately distributed on the semiconductor material slab and the molecules, resulting in a reduced rate of their composite reaction. Therefore, the midgap energy levels generated by adsorptive molecules can induce electron transfer paths to produce efficient photogenerated electrons, so as to improve the efficiency of visible light degradation of pollutants. However, in our degradation experiments, benzene and ethyl acetate did not show significant degradation under visible light irra-

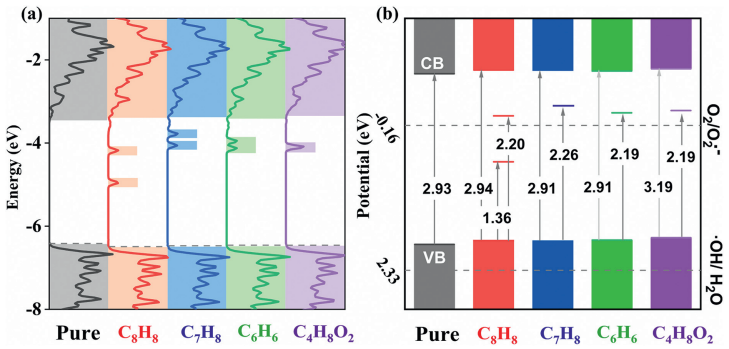

Fig. 7. The DOS for the pristine and VOCs molecules adsorbed $BaTiO_3$ (001) surfaces. (a) The energy zero shifts to the vacuum level and the Fermi level are represented as a dashed line. (b) Diagram of energy with respect to vacuum as well as potential *versus* the normal hydrogen electrode (pH = 7.0, 0 V *vs.* NHE ~ −4.5 eV) of surface in both pristine and adsorbing $BaTiO_3$ (001) surface. The chemical potential generated by $^{\bullet}OH$ and $O_2^{\bullet-}$ is marked in the figure. (−0.16/2.33 eV, $^{\bullet}OH/O_2^{\bullet-}$). The color line between CB and VB represents the intermediate gap state generated by VOCs adsorption.

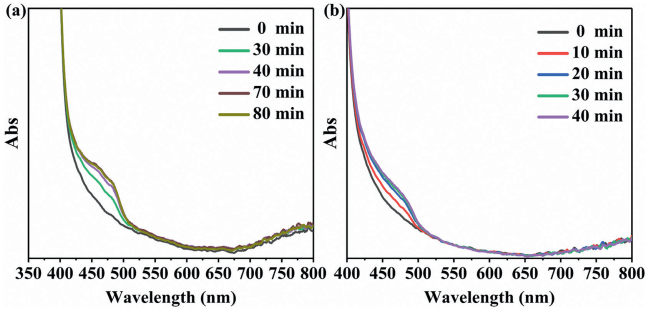

Fig. 8. *In situ* UV–vis absorption spectra of $BaTiO_3$ during continuous adsorption of (a) styrene and (b)toluene.

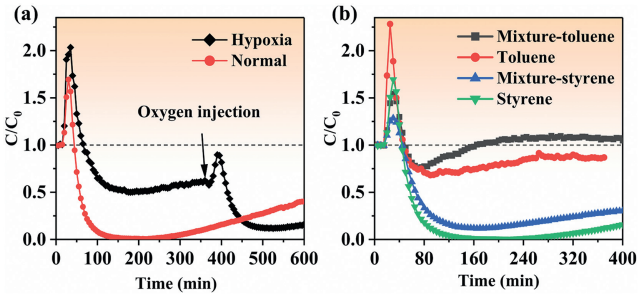

Fig. 9. (a) Degradation kinetics of styrene, ethyl acetate, their mixture-styrene, and their mixture-ethyl acetate by $BaTiO_3$ under visible light. (b) Comparative degradation kinetics of styrene by $BaTiO_3$ under anaerobic and aerobic conditions in the presence of visible light.

diation through $BaTiO_3$ (Fig. 1a). This may be due to the fact that even though benzene and ethyl acetate adsorbed on the $BaTiO_3$ surface generate a bandgap that can utilize visible light, the photocatalytic reaction is significantly influenced by the recombination rate of electron-hole pairs and the lifetime of the reactive species.

In summary, the adsorption of VOCs molecules can cause self-sensitization of semiconductor materials under visible light, enhancing photocatalytic efficiency of the surface. The performance of self-sensitization is dependent on the local midgap condition caused by VOC adsorption. The local midgap state can drive photocharge transfer from VOC molecules to the investigated semiconductor, consequently narrowing the surface band gap.

To further validate the accuracy and reliability of DFT calculations, an *in situ* UV–vis experiment was implemented to explore the dynamic changes in the UV–vis absorption spectra of $BaTiO_3$ during the adsorption of styrene or toluene. As shown in Fig. 8, in the visible range of 410–500 nm, the light absorption intensity of $BaTiO_3$ gradually increased with the extension of the adsorption time for styrene or toluene. Notably, these observations are highly consistent with experimental data on the degradation of styrene by $BaTiO_3$ under different visible light wavelengths. This experimental result confirms that the adsorption of styrene or toluene onto the surface of $BaTiO_3$ significantly impacts its light absorption characteristics. This may be the main reason for triggering the obvious degradation reaction in the visible range. The results show a high degree of consistency with DFT computational results (Fig. S1 in Supporting information).

DFT calculation results show that VOCs are not significantly degraded when VOCs get electrons (Table S1 in Supporting information). Furthermore, an oxygen-free styrene diluted with nitrogen was used for the photocatalytic degradation of $BaTiO_3$ under visible light. As illustrated in Fig. 9a, the degradation under anoxic conditions persisted for only an initial period of 350 min, a sharp deviation from the ongoing degradation seen under aerobic conditions. This outcome can probably be ascribed to the residual oxygen initially adsorbed on the catalyst surface, which got progressively depleted over the first 350 min. When oxygen was reintroduced into the system at the 360 min mark, the degradation rate of styrene reverted to its optimal level. This suggests that oxygen may play a key role in the degradation of VOCs. The oxygen may be converted into superoxide radicals to participate in further reactions.

To further probe the possibility of superoxide radical generation in the aforementioned degradation process, a more intricate experimental setup was devised. Superoxide radicals are highly reactive free radicals capable of indiscriminately attacking various VOCs with almost no difference in their reaction rates. In this experiment, a mixture of VOCs containing styrene and toluene was subjected to visible-light catalysis and exposed to a $BaTiO_3$ catalyst. As depicted in Fig. 9b, the degradation performance of toluene in isolation did not exhibit significant differences when compared to its performance in the mixed VOCs. Notably, the degradation efficacy of both styrene and toluene in the mixed VOCs was marginally lower than that of the individual VOCs. This observation suggests that superoxide radicals may not generated during this degradation process. Therefore, it demonstrated that the degradation process does not involve the generation of superoxide radicals, offering further insights into the mechanistic understanding of VOCs degradation.

A non-traditional gas-solid photocatalytic process was proposed based on the experimental and theoretical results. The adsorption of VOCs leads to an interaction between the ground state of VOCs and the valence band position of the semiconductor, thereby form-

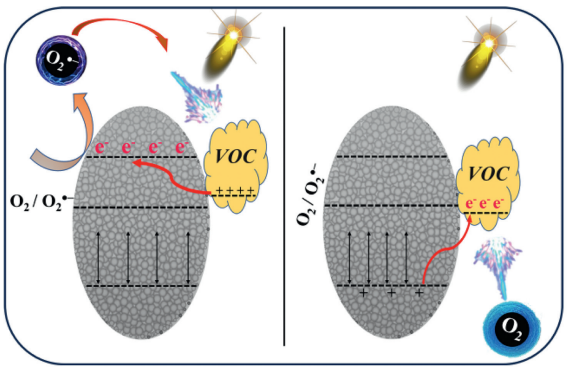

Fig. 10. Mechanism diagram of visible light-induced degradation of VOCs using wide-bandgap semiconductor.

ing a new band gap. Under the condition of visible light irradiation, this newly formed band gap prompts electrons to transfer from valence band of the semiconductor to the VOCs. These electron-enriched VOCs subsequently react with oxygen, facilitating the degradation of VOCs (Fig. 10).

In this study, a novel photocatalytic mechanism was discovered, where photo-electrons directly transfer from the valence band of wide-bandgap semiconductors to VOCs. In this mechanism, the generation of photo-electrons is due to the formation of an intermediate bandgap that can utilize visible light between the valence band of the semiconductor catalyst and the VOCs adsorbed on its surface. This differs from the traditional band theory that relies on the bandgap width of the semiconductor to utilize light energy. Moreover, in previous studies, an intermediate bandgap was formed between VOCs and the conduction band of the catalyst semiconductor that could utilize visible light. Photogenerated electrons were transferred from VOCs to the conduction band of the semiconductor, which is different from this work. This work not only enriches the existing theoretical framework for non-traditional gas-solid photocatalytic degradation of VOCs but also provides a more comprehensive understanding of the field. It is anticipated to further advance the development of non-traditional gas-solid photocatalysis in environmental protection and facilitating the industrial applications of photocatalytic degradation of VOCs.

Declaration of competing interest

The authors declare that they have no known competing financial interests or personal relationships that could have appeared to influence the work reported in this paper.

CRediT authorship contribution statement

Teng Wang: Conceptualization, Data curation, Methodology, Writing – original draft. **Jiachun Cao:** Methodology, Software, Writing – original draft. **Juan Li:** Methodology, Supervision, Writing – review & editing. **Didi Li:** Supervision, Writing – review & editing. **Zhimin Ao:** Funding acquisition, Project administration, Supervision, Writing – review & editing.

Acknowledgments

This work was financially supported by the National Natural Science Foundation of China (No. 22176041, T2421005), National Key R&D Program of China (No. 2022YFC3901800), the Fundamental Research Funds for the Central Universities (No. 2243200011), and Guangzhou Science and Technology Planning Project (No. 2023A04J0918).

Supplementary materials

Supplementary material associated with this article can be found, in the online version, at doi:10.1016/j.cclet.2024.110078.

References

[1] K. Zhang, H. Ding, W. Pan, et al., Environ. Sci. Technol. 56 (2022) 9220–9236.
[2] Y. Zheng, K. Fu, Z. Yu, et al., J. Mater. Chem. A 10 (2022) 14171–14186.
[3] Y. Zhu, W. Zhao, B. Jing, et al., Chin. Chem. Lett. 34 (2023) 107816.
[4] S. Meng, Y. Li, Y. Liu, et al., Env. Surf. Interf. 1 (2023) 10–23.
[5] W. Gao, X. Zhang, X. Su, et al., Chem. Eng. J. 346 (2018) 77–84.
[6] D.M. Tobaldi, D. Dvoranová, L. Lajaunie, et al., Chem. Eng. J. 405 (2021) 126651.
[7] J. Zhang, Y. Hu, J. Qin, Z. Yang, M. Fu, Chem. Eng. J. 385 (2020) 123814.
[8] L. Qiu, Y. Wang, H. Li, et al., Catalysts 8 (2018) 596.
[9] M. Krichevskaya, S. Preis, A. Moiseev, N. Pronina, J. Deubener, Catal. Today 280 (2017) 93–98.
[10] B.M. da Costa Filho, V.J.P. Vilar, Chem. Eng. J. 391 (2020) 123531.
[11] T. Wang, C. Nie, Z. Ao, S. Wang, T. An, J. Mater. Chem. A 8 (2020) 485–502.
[12] E.F. Mohamed, G. Awad, Environ. Sci. Pollut. Res. 27 (2020) 24507–24517.
[13] J.J. Li, M. Zhang, B. Weng, et al., Appl. Surf. Sci. 507 (2020) 145133.
[14] Y. Shu, M. He, J. Ji, et al., J. Hazard. Mater. 364 (2019) 770–779.
[15] H. Anwer, M. Ali, S. Lee, S.H. Jeong, J.W. Park, J. Hazard. Mater. 409 (2021) 124497.
[16] Y. Naciri, A. Hsini, Z. Ajmal, et al., Adv. Colloid Interface Sci. 280 (2020) 102160.
[17] C.Q. Ma, N. Han, R.Z. Zhang, et al., Env. Sur. Interf. 1 (2023) 3–9.
[18] T. Wang, J. Cao, J. Li, et al., Environ. Sci.: Nano 11 (2024) 2415–2427.
[19] Q. Liu, W. Zhao, Z. Ao, T. An, Chin. Chem. Lett. 33 (2022) 410–414.
[20] S.K. Ray, J. Cho, J. Hur, J. Environ. Manage. 290 (2021) 112679.
[21] G. Kresse, J. Furthmüller, Comput. Mater. Sci. 6 (1996) 15–50.
[22] J.P. Perdew, K. Burke, Y. Wang, Phys. Rev. B: Condens. Matter Mater. Phys. 54 (1996) 16533–16539.
[23] S. Grimme, S. Ehrlich, L. Goerigk, J. Comput. Chem. 32 (2011) 1456–1465.
[24] G. Masresha, S.A. Jabasingh, S. Kebede, D. Doo-Arhin, M. Assefa, Can. J. Chem. Eng. 101 (2023) 6905–6918.
[25] M. Boulos, S. Guillemet-Fritsch, F. Mathieu, et al., Solid State Ionics 176 (2005) 1301–1309.
[26] P. Demircivi, B. Gulen, E.B. Simsek, D. Berek, Mater. Chem. Phys. 241 (2020) 122236.
[27] K.K.Pant Sonal, S. Upadhyayula, Fuel 276 (2020) 118044.
[28] V.La Parola, G. Deganello, S. Scirè, A.M. Venezia, J. Solid State Chem. 174 (2003) 482–488.
[29] H. Wang, B. Xiao, X. Cheng, et al., Appl. Catal. A 502 (2015) 157–165.